A UNITED STATES DEPARTMENT OF COMMERCE PUBLICATION

NBS TECHNICAL NOTE 390

Far Infrared Absorption in Liquefied Gases

U. S. DEPARTMENT OF COMMERCE
National Bureau of Standards

NATIONAL BUREAU OF STANDARDS

The National Bureau of Standards [1] was established by an act of Congress March 3, 1901. Today, in addition to serving as the Nation's central measurement laboratory, the Bureau is a principal focal point in the Federal Government for assuring maximum application of the physical and engineering sciences to the advancement of technology in industry and commerce. To this end the Bureau conducts research and provides central national services in four broad program areas. These are: (1) basic measurements and standards, (2) materials measurements and standards, (3) technological measurements and standards, and (4) transfer of technology.

The Bureau comprises the Institute for Basic Standards, the Institute for Materials Research, the Institute for Applied Technology, the Center for Radiation Research, the Center for Computer Sciences and Technology, and the Office for Information Programs.

THE INSTITUTE FOR BASIC STANDARDS provides the central basis within the United States of a complete and consistent system of physical measurement; coordinates that system with measurement systems of other nations; and furnishes essential services leading to accurate and uniform physical measurements throughout the Nation's scientific community, industry, and commerce. The Institute consists of an Office of Measurement Services and the following technical divisions:

Applied Mathematics—Electricity—Metrology—Mechanics—Heat—Atomic and Molecular Physics—Radio Physics [2]—Radio Engineering [2]—Time and Frequency [2]—Astrophysics [2]—Cryogenics.[2]

THE INSTITUTE FOR MATERIALS RESEARCH conducts materials research leading to improved methods of measurement standards, and data on the properties of well-characterized materials needed by industry, commerce, educational institutions, and Government; develops, produces, and distributes standard reference materials; relates the physical and chemical properties of materials to their behavior and their interaction with their environments; and provides advisory and research services to other Government agencies. The Institute consists of an Office of Standard Reference Materials and the following divisions:

Analytical Chemistry—Polymers—Metallurgy—Inorganic Materials—Physical Chemistry.

THE INSTITUTE FOR APPLIED TECHNOLOGY provides technical services to promote the use of available technology and to facilitate technological innovation in industry and Government; cooperates with public and private organizations in the development of technological standards, and test methodologies; and provides advisory and research services for Federal, state, and local government agencies. The Institute consists of the following technical divisions and offices:

Engineering Standards—Weights and Measures — Invention and Innovation — Vehicle Systems Research—Product Evaluation—Building Research—Instrument Shops—Measurement Engineering—Electronic Technology—Technical Analysis.

THE CENTER FOR RADIATION RESEARCH engages in research, measurement, and application of radiation to the solution of Bureau mission problems and the problems of other agencies and institutions. The Center consists of the following divisions:

Reactor Radiation—Linac Radiation—Nuclear Radiation—Applied Radiation.

THE CENTER FOR COMPUTER SCIENCES AND TECHNOLOGY conducts research and provides technical services designed to aid Government agencies in the selection, acquisition, and effective use of automatic data processing equipment; and serves as the principal focus for the development of Federal standards for automatic data processing equipment, techniques, and computer languages. The Center consists of the following offices and divisions:

Information Processing Standards—Computer Information — Computer Services — Systems Development—Information Processing Technology.

THE OFFICE FOR INFORMATION PROGRAMS promotes optimum dissemination and accessibility of scientific information generated within NBS and other agencies of the Federal government; promotes the development of the National Standard Reference Data System and a system of information analysis centers dealing with the broader aspects of the National Measurement System, and provides appropriate services to ensure that the NBS staff has optimum accessibility to the scientific information of the world. The Office consists of the following organizational units:

Office of Standard Reference Data—Clearinghouse for Federal Scientific and Technical Information [3]—Office of Technical Information and Publications—Library—Office of Public Information—Office of International Relations.

---

[1] Headquarters and Laboratories at Gaithersburg, Maryland, unless otherwise noted; mailing address Washington, D.C. 20234.
[2] Located at Boulder, Colorado 80302.
[3] Located at 5285 Port Royal Road, Springfield, Virginia 22151.

UNITED STATES DEPARTMENT OF COMMERCE
Maurice H. Stans, Secretary
NATIONAL BUREAU OF STANDARDS ● Lewis M. Branscomb, Director

TECHNICAL NOTE 390

ISSUED APRIL 1970

Nat. Bur. Stand. (U.S.), Tech. Note 390, 39 pages (April 1970)
CODEN: NBTNA

Far Infrared Absorption in Liquefied Gases

M. C. Jones

Cryogenics Division
Institute for Basic Standards
National Bureau of Standards
Boulder, Colorado 80302

NBS Technical Notes are designed to supplement the Bureau's regular publications program. They provide a means for making available scientific data that are of transient or limited interest. Technical Notes may be listed or referred to in the open literature.

For sale by the Superintendent of Documents, U.S. Government Printing Office, Washington, D.C. 20402
(Order by SD Catalog No. C13.46:390), Price 50 cents

CONTENTS

		page
1.	Introduction	1
2.	Experimental	2
	2.1 The spectrophotometer	2
	2.2 Optical dewar and liquid absorption cells	2
	2.3 Thermometry and temperature control	9
	2.4 Liquid samples	11
	2.5 Experimental procedure	12
3.	Results	13
	3.1 Data reduction	13
	3.2 Errors	19
4.	Discussion	21
	4.1 Liquid hydrogen	21
	4.2 Liquid nitrogen	23
	4.3 Liquid oxygen	27
	4.4 Liquid carbon monoxide	31
	4.5 Liquid methane	31
	4.6 Liquid argon	33
5.	Applications - Absorption of thermal radiation	33
6.	Conclusions	35
7.	Acknowledgments	36
8.	References	37

LIST OF FIGURES

		page
Figure 1.	Schematic Arrangement	3
Figure 2.	Optical Dewar	4
Figure 3.	Absorption Cell-Quartz Windows. Path Length Variable from 4.1 mm to 25.4 mm	5
Figure 4.	Absorption Cell-Polyethylene Windows. Path Length 32.5 mm. The Cell is Shown Inserted in the Reflux Channel Yoke	6
Figure 5.	Absorption Cell-Polyethylene Windows. Path Length 5.9 mm.	8
Figure 6.	Temperature Measurement and Control System. .	10
Figure 7.	Schematic of Possible Paths Through a Typical Absorption Cell	15
Figure 8.	Far Infrared Absorption in Liquid Hydrogen-Translational Band	22
Figure 9.	Far Infrared Absorption in Liquid Hydrogen-Rotational Band	24
Figure 10.	Far Infrared Absorption in Liquid Nitrogen . . .	25
Figure 11.	Far Infrared Absorption in Liquid Oxygen	26
Figure 12.	Far Infrared Absorption in Liquid Carbon Monoxide	30
Figure 13.	Far Infrared Absorption in Liquid Methane	32

FAR INFRARED ABSORPTION IN LIQUEFIED GASES *

M. C. Jones
Cryogenics Division
Institute for Basic Standards, National Bureau of Standards
Boulder, Colorado

ABSTRACT

Experimental results are given for the absorption coefficient of the liquids hydrogen (three para concentrations), nitrogen, oxygen, carbon monoxide, methane and argon in the wavenumber range 20-250 cm^{-1} (40-500 μm). In addition, data for liquid hydrogen are given at wave numbers up to 600 cm^{-1} (16.7 μm). The results are discussed in terms of the induced dipole, and, in the case of carbon monoxide, the permanent dipole. An indication of the way in which the data may be employed in calculations of thermal radiative transfer is made by calculation of the modified Planck mean absorption coefficient.

Key Words: Far infrared; absorption coefficient; liquefied gases; hydrogen; nitrogen; oxygen; carbon monoxide; methane; argon.

* This work was performed at the National Bureau of Standards under the sponsorship of the National Aeronautics and Space Administration, Space Nuclear Propulsion Office, Fund Transfer R-45.

1. INTRODUCTION

Absorption spectra of simple molecules in the far infrared are generally related to rotational transitions. For transitions involving permanent dipole moments the effect of increase of density is to broaden the rotational lines. However, at sufficiently high densities absorption also occurs in non-polar species where none had been apparent at low densities. Such absorption is well known (e.g. Bosomworth and Gush, 1965) and is attributed to electric dipole moments induced on collision by the quadrupole and higher multipole fields of neighboring molecules. It is conveniently studied at liquid densities where path lengths of a few centimeters are sufficient for observation. Unfortunately, as with other phenomena dependent on collisions none of the theory of induced absorption is applicable at these densities so that the resulting spectra do not yield molecular constants (e.g. quadrupole moments). Nevertheless, because the spectra result exclusively from the molecular interactions of the liquid state it was felt that an exploratory investigation of several simple molecular species would be useful apart from the value of such reference data as might result.

In this report we present the far infrared spectra of liquids hydrogen (three different para-hydrogen concentrations), nitrogen, oxygen, methane, and carbon monoxide. In addition, we have examined liquid argon in our absorption cell and verified that within the uncertainty limits of our experiments it does not absorb. Since the work involved the solution of several problems peculiar to this type of measurement we give a fairly full account of experimental details (sections 2 and 3). In section 4 the experimental results are presented and discussed and in section 5 we indicate briefly the application of the data in calculations of thermal radiative transfer.

2. EXPERIMENTAL

2.1 The Spectrophotometer

The spectrophotometer could be used with conventional globar or high pressure mercury lamp sources, crystal choppers, reststrahlen and wire mesh reflection filters. The monochromator had an aperture ratio of $f/3.8$ and used Littrow mounted gratings in first order in a single pass arrangement. The detector was a Golay cell. In all measurements reported here the instrument was used in single beam operation using a lock-in amplifier to drive a chart recorder with reference signal taken from a breaker on the chopper drive (see figure 1.) For all measurements the instrument was kept purged with dry nitrogen gas from a boiling liquid nitrogen reservoir.

2.2 Optical Dewar and Liquid Absorption Cells.

A special dewar, figure 2, was constructed to enable liquid cells to be held at predetermined temperatures. In all experiments liquid hydrogen was used as refrigerant in the inner container and a liquid cell was attached at the lower end of the reflux tube — a thin-walled stainless steel tube passing through the refrigerant container. Variable thermal conductance between the refrigerant and the liquid cell could be obtained by variation of hydrogen gas pressure inside the reflux tube. The liquid cell was surrounded by a nitrogen-temperature radiation shield except for holes to allow the passage of the spectrophotometer beam. When liquid hydrogen was used as sample, a second hydrogen-temperature shield attached to the refrigerant bath was used. The outer vacuum jacket of the dewar was fitted with 1/8" thick polyethylene windows.

Two choices of window are available in the far infrared, namely: crystal quartz and polyethylene. Polyethylene is desirable on account

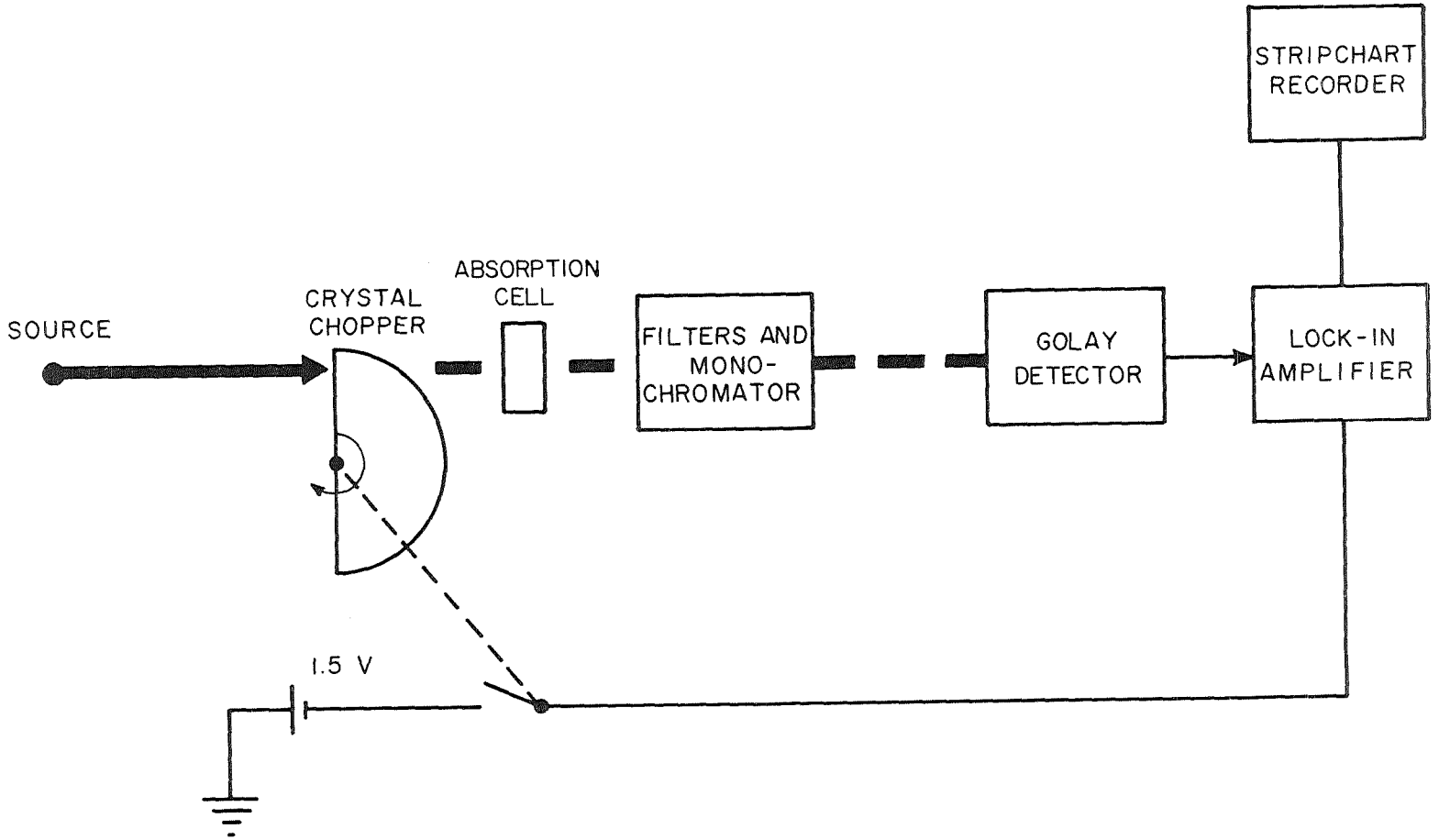

Figure 1. Schematic Arrangement.

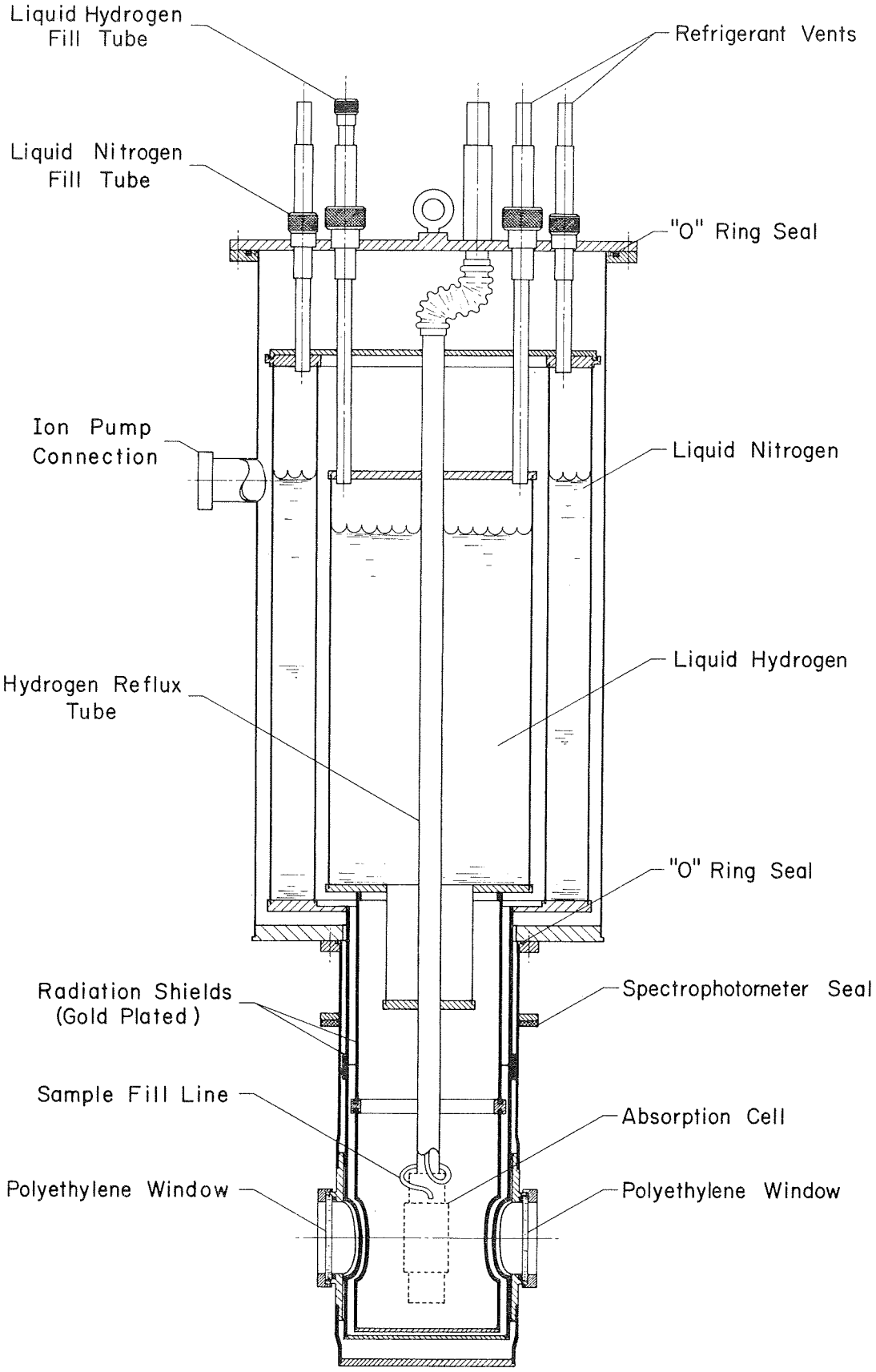

Figure 2. Optical Dewar.

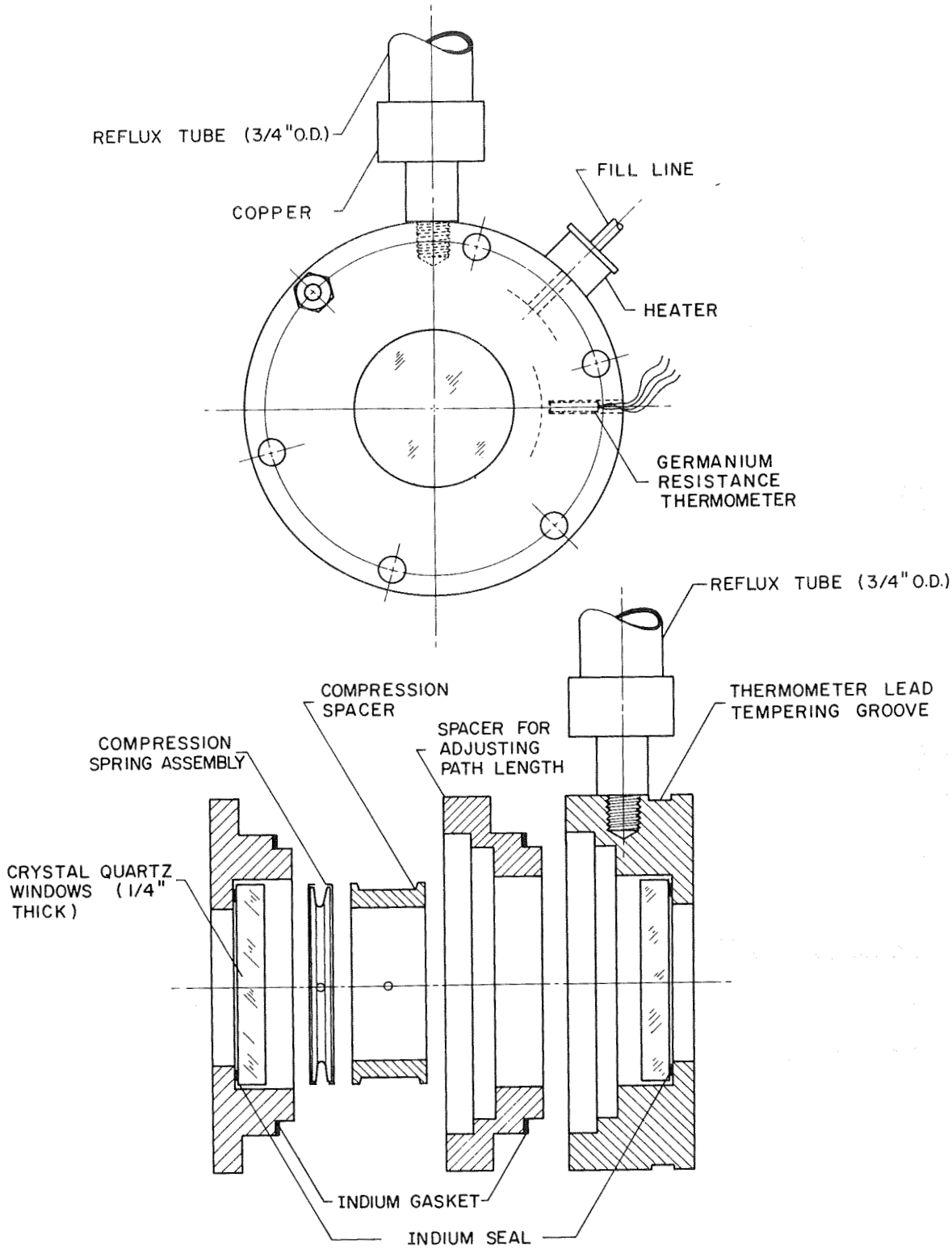

Figure 3. Absorption Cell-Quartz Windows. Path Length Variable from 4.1 mm to 25.4 mm.

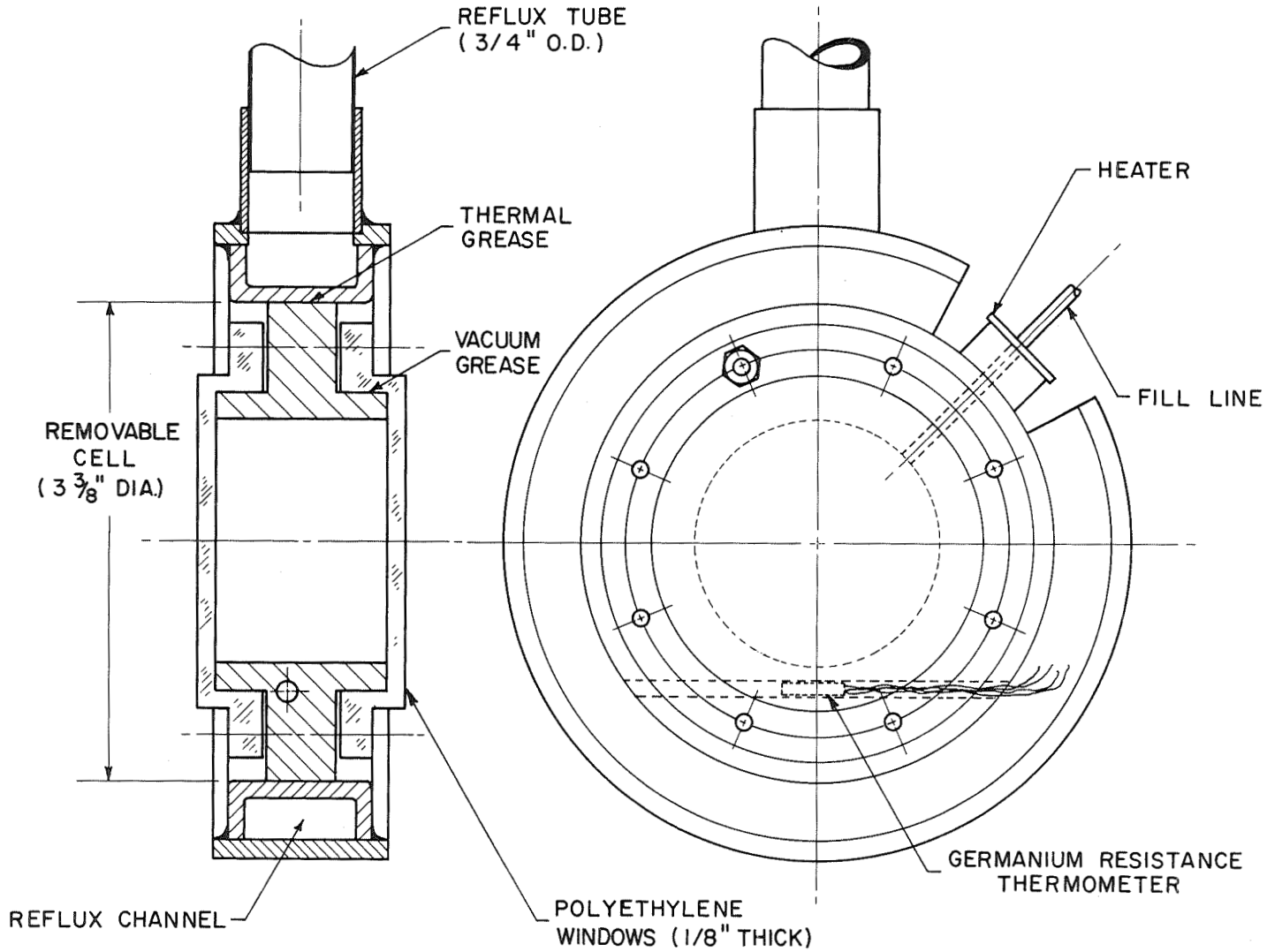

Figure 4. Absorption Cell-Polyethylene Windows. Path Length 32.5 mm. The Cell is Shown Inserted in the Reflux Channel Yoke.

of its wide spectral range as a window (0 to 600 cm^{-1}) and again on account of the low reflectance loss at a polyethylene/vacuum interface (about 5%). However, it is less satisfactory than quartz where window rigidity is important. Our earlier attempts at making vacuum tight low temperature liquid cells with polyethylene windows were, however, unsuccessful due to its excessive shrinkage on cooling, and so experiments were begun using the cell of figure 3. This cell was fitted with crystal quartz windows cut perpendicular to the x or y axes. Crystal quartz is readily sealed using indium wire as a gasket material. However, we found that a spring load on the seal was required to maintain the seal through temperature cycles. This was achieved by use of the 'U' cross section steel spring ring shown in the figure. With it a force of 200 pounds was continually maintained against the window seal. The path length of this cell could be changed from 12.7 to 25.4 mm by the inclusion of the spacer shown. For an even shorter path length, 4.1 mm, one window could be raised by including a spacer between window and seat.

The cell of figure 3 was used for all experiments on liquids nitrogen, oxygen, methane, carbon monoxide, and argon and some preliminary runs with hydrogen. It had a usable wave number range from 0 to 250 cm^{-1} and an almost constant reflectance of 15 percent was measured at a vacuum/quartz interface in this range.

For measurements on liquid hydrogen, where much of the interest is at wave numbers beyond 250 cm^{-1}, we eventually designed a successful polyethylene window seal and this is embodied in the cell shown in figure 4. This cell had a path length of 32.5 mm and could be used where the absorption coefficient was less than about 1 cm^{-1}. The polyethylene windows are forced over the drum forming the cell body with vacuum grease as sealant. On cooling down, the outer flange

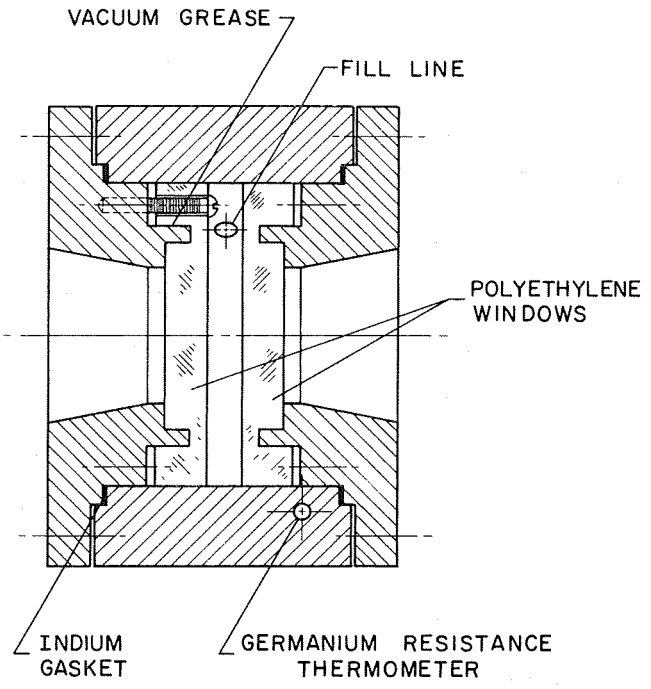

Figure 5. Absorption Cell-Polyethylene Windows. Path Length 5.9 mm.

shrinks on to the drum forming an ever tighter seal. Whereas the cell of figure 3 could be simply screwed to the end of the reflux tube, in order to obtain low enough temperatures for hydrogen liquid samples in this cell we found it necessary to extend the reflux tube in the form of a channel around the cell. The cell body then simply slides into the yoke formed by this channel. Thermal contact with the channel was maintained by use of a zinc-oxide-filled silicone grease.

For short path lengths and higher pressures the design of figure 5 was used in which the same window sealing principle is embodied, but now pressure in the cell acts to seal it further. This cell can also be slid into the reflux channel yoke of figure 4. The path length was 5.9 mm.

All cells were fitted with a single 1/8" diameter copper fill line, a 40 Ω heater and a well to receive a germanium resistance thermometer bulb. When liquid hydrogen was to be condensed into a cell, the fill time was shortened considerably by routing the fill line down through the reflux tube, thereby precooling the incoming gas before it entered the cell. For all other samples, the fill line remained on the outside of the radiation shields.

2.3 Thermometry and Temperature Control

Temperatures of the sample cells were measured with the germanium resistance thermometer. This had received a manufacturer's calibration, but due to the irreproducibility of the resistance we checked it against temperatures obtained by measuring vapor pressures of sample liquids in half filled cells. This was done with liquids nitrogen methane and hydrogen. From our vapor pressure determinations we feel that temperatures quoted are within 0.1 K, which is sufficient for these experiments.

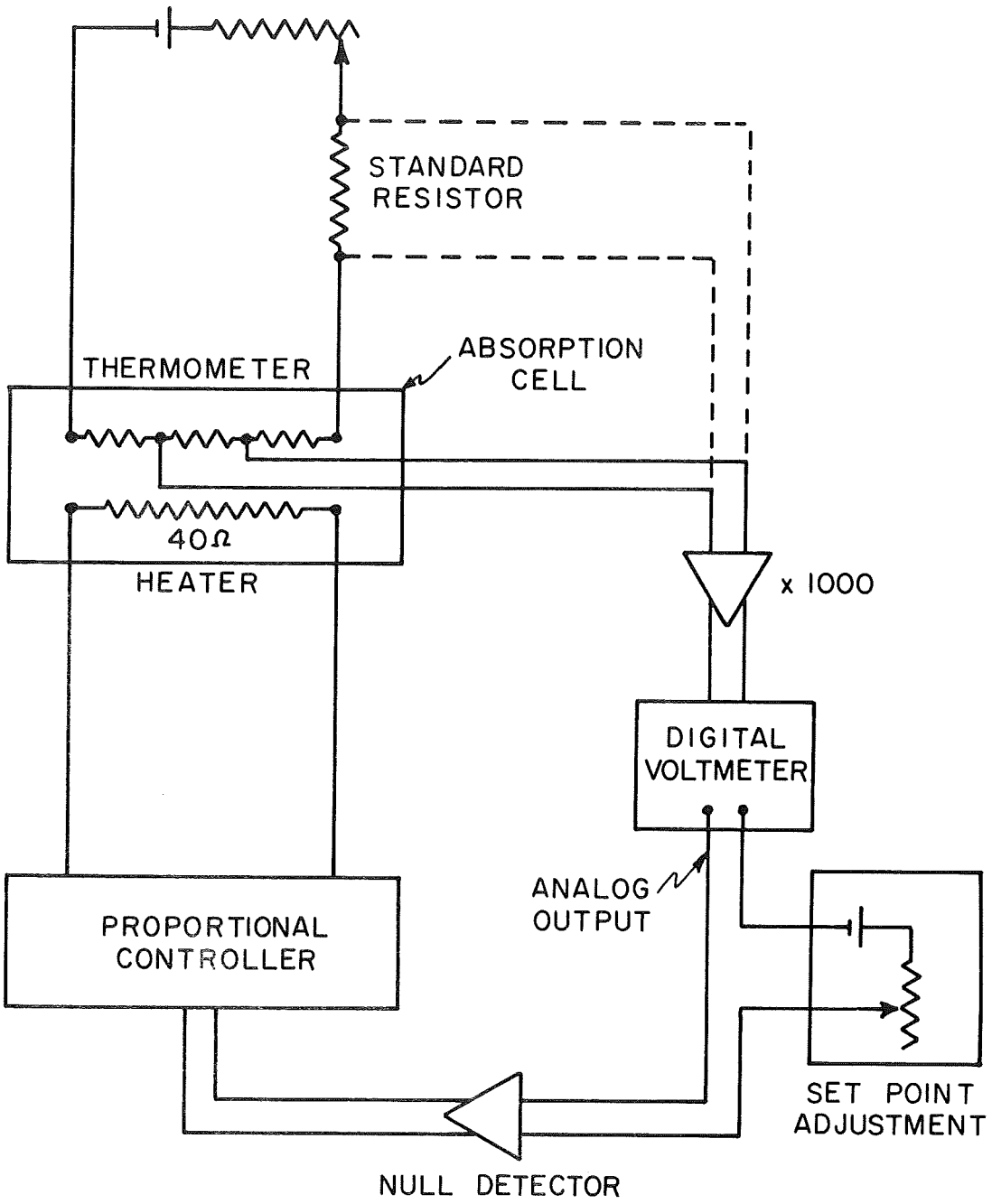

Figure 6. Temperature Measurement and Control System.

Much more important than the absolute value of the temperature itself when using quartz windows in the cell is the stability of the cell temperature. The transmission of the quartz is quite temperature sensitive above about 25 K so it is necessary to make transmission measurements with cell empty and cell full at temperatures within about 0.1 K of each other. With the control system shown schematically in figure 6, control within a few hundredths of a degree was easily achieved. The same thermometer as is used to indicate temperature via the amplifier and digital voltmeter is also used to drive the controller by making use of an isolated analog output of the digital voltmeter.

2.4 Liquid Samples

All samples, regardless of their origin were passed through a synthetic zeolite bed at room temperature before entering the cell to guard against possible moisture inclusion.

Normal hydrogen was obtained from a gas cylinder which was known to have been filled several years previously with para-hydrogen from storage boil-off gas. Such cylinders are known to be as pure as the best commercial high purity hydrogen.

Para-hydrogen was obtained from the boil-off of our refrigerant. Its composition was found with a thermal conductivity analyzer to be identical to samples which had been prepared by passing normal hydrogen over an iron oxide catalyst at 20 K and is therefore considered to be essentially equilibrium hydrogen at 20 K, i.e., 99.8 percent parahydrogen.

An intermediate concentration of parahydrogen was obtained by passing normal hydrogen through an iron oxide catalyst held in a liquid nitrogen bath. This method produced a composition which varied

somewhat with flow rate as determined on the thermal conductivity analyzer. At the flow rates used in filling our liquid cell a composition of from 44 to 48 percent parahydrogen was indicated.

Nitrogen was obtained as boil-off gas from commercial liquid for which the manufacturers analysis showed a typical purity of 99.997 percent.

Oxygen, methane, carbon monoxide, and argon were all obtained from cylinders with manufacturers purity specifications of 99.5, 99.95, 99.5, and 99.996 percent respectively.

2.5 Experimental Procedure

Prior to taking data, the dewar was placed in the spectrophotometer and with all power on the assembly was allowed to reach steady operating conditions.

With the absorption cell evacuated and cooled down to the required temperature, the transmitted signal was recorded for each of about 8 frequencies. At each frequency the signal was recorded when steady for up to five minutes with suitable filtering (up to a time constant of 100 secs). After this the sample gas was admitted to the cell and condensed in. This process was monitored by both gas flow rate and by continuously recording the signal at a particular frequency; the signal reduced until the beam became completely submerged.

When gas flow had stopped the cell was returned to its original temperature and the signal recorded again at each of the chosen frequencies. On conclusion, the cell was evacuated and again returned to its original temperature to check the original cell empty readings. Readings were repeated unless the cell empty readings agreed to within 2 percent.

Finally, at each of the amplifier gain settings used, the signal was recorded with the spectrophotometer slit closed. This was necessary due to the tendency of the Golay cell to pick up mechanical vibration from the chopper and breakers, which being in constant phase relation to the light signal, appear as a false signal. The resulting offset from the recorder zero is thus a function of the amplifier gain setting.

3. RESULTS

3.1 Data Reduction

In deriving the absorption coefficient, α, from the recorded signals one must take into account the phenomenon of dielectric mismatch at the window/liquid and window/vacuum interfaces and the resulting multiple reflections between pairs of parallel interfaces. In our case the multiple reflections would not give rise to observable interference effects as may easily be shown.

The resonant condition for parallel interfaces separated by a distance d is

$$d = \frac{m\lambda}{2}$$

where m is an integer and λ the wavelength. For adjacent resonant wavelengths

$$\frac{\Delta\left(\frac{1}{\lambda}\right)}{\Delta m} = \frac{1}{2d} \quad , \qquad \Delta m = 1$$

In our experiments the smallest value of d was about 3 mm, therefore resonance separation $\Delta\left(\frac{1}{\lambda}\right)$ is about 1.6 cm^{-1} at the most. Most of the data reported here were taken with a spectral slit width approaching 10 cm^{-1} so that each recorded signal represents an average of several resonances and none would be observed.

The total intensity at the detector may be calculated by summing the intensities from every possible path through the cell. Referring to figure 7, let E_{ijk} and I_{ijk} be the amplitude and intensity of an emerging ray from a path in which there were i double reflections inside the first window, j double reflections between the windows and k double reflections inside the second window. Let E_0 and I_0 be the incident amplitude and intensity respectively and let the amplitude transmission coefficients be t_{01} for a vacuum/window interface, t_{12} for a window/liquid interface and t_{21} and t_{10} the corresponding coefficients for the reverse order of the media. With the same subscript notation $r_{\ell m}$ represents the appropriate amplitude reflection coefficient. Then for a general ray the transmitted amplitude is

$$E_{ijk} = E_0 t_{01} \left(r_{10} r_{12}\right)^i t_{12} r_{21}^{2j} e^{-(2j+1)\frac{\alpha}{2}\ell} t_{21} \left(r_{12} r_{10}\right)^k t_{10} \qquad (1)$$

The contribution to the intensity from this ray is

$$I_{ijk} = E_0^2 t_{01}^2 \left(r_{10} r_{12}\right)^{2i} t_{12}^2 r_{21}^{4j} e^{-(2j+1)\alpha\ell} t_{21}^2 \left(r_{12} r_{10}\right)^{2k} t_{10}^2 \qquad (2)$$

The total intensity transmitted through the cell is obtained by summing over i j and k from zero to infinity:

$$I_T = \sum_i \sum_j \sum_k I_{ijk} \qquad (3)$$

or

$$\frac{I_T}{I_0} = \frac{t_{01}^2 t_{12}^2 t_{21}^2 t_{10}^2 e^{-\alpha\ell}}{\left(1-r_{10}^2 r_{12}^2\right)\left(1-r_{21}^4 e^{-2\alpha\ell}\right)\left(1-r_{10}^2 r_{12}^2\right)} \qquad (4)$$

The transmittances T and reflectances R at the interfaces can now be introduced and related to the transmission coefficients via the refractive indeces, n, as follows:

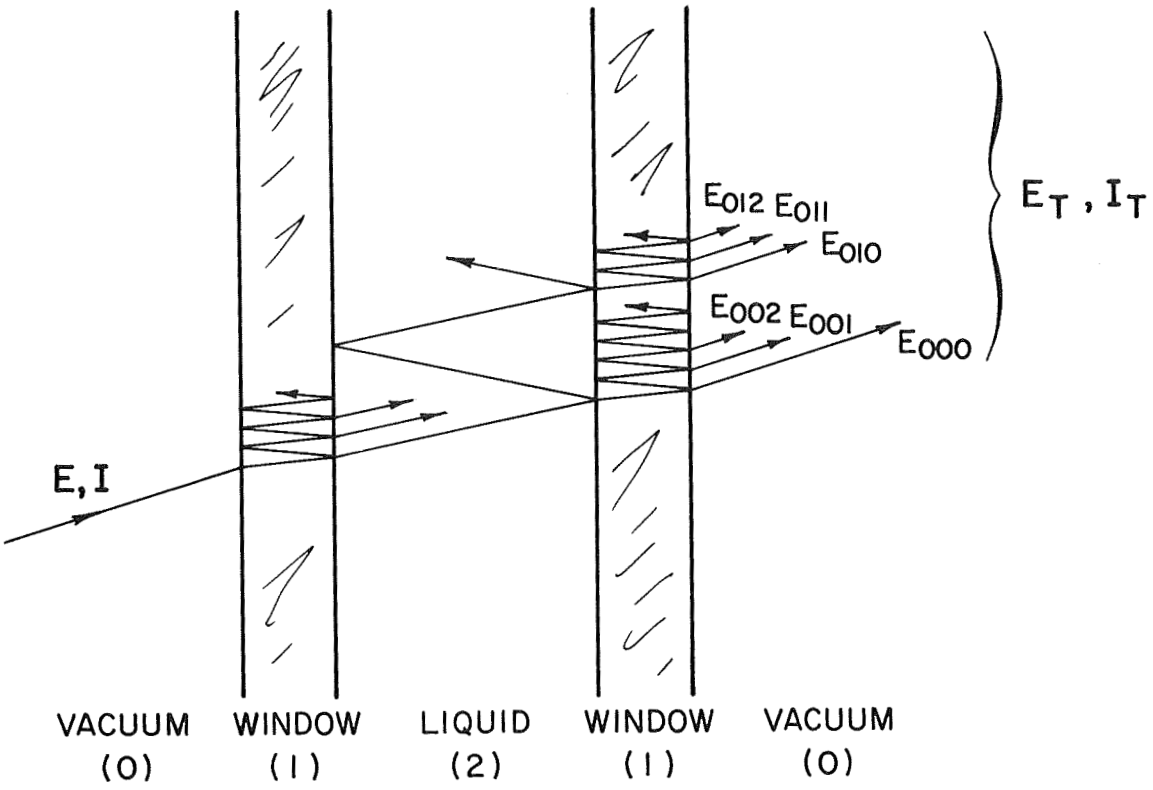

Figure 7. Schematic of Possible Paths Through a Typical Absorption Cell.

$$T_{01} = \frac{n_1}{n_0} t_{01}^2 \quad , \quad T_{12} = \frac{n_2}{n_1} t_{12}^2 \tag{5}$$

$$T_{21} = \frac{n_1}{n_2} t_{21}^2 \quad , \quad T_{10} = \frac{n_0}{n_1} t_{10}^2$$

Whereas for the reflectances

$$R_{10} = r_{10}^2 \quad , \quad R_{12} = r_{12}^2 \quad \text{etc.} \tag{6}$$

We note also that $T_{01} = 1-R_{01}$ etc. The refractive index ratios all cancel upon substitution of (5) and (6) into (4) giving

$$\frac{I_T}{I_0} = \frac{\left(1-R_{10}\right)^2 \left(1-R_{12}\right)^2 e^{-\alpha \ell}}{\left(1-R_{10}R_{12}\right)^2 \left(1-R_{12}^2 e^{-2\alpha\ell}\right)} \tag{7}$$

The corresponding transmitted intensity I'_T for the evacuated cell is immediately obtained from (7) on replacing the subscript 2 by 0 giving

$$\frac{I'_T}{I_0} = \frac{\left(1-R_{10}\right)^4}{\left(1-R_{10}^2\right)^2 \left(1-R_{10}^2\right)} \tag{8}$$

On dividing (7) by (8) and taking logarithms

$$\alpha = \frac{1}{\ell} \left\{ \ln \left[\frac{\left(1-R_{12}\right)^2 \left(1-R_{10}^2\right)^2 \left(1-R_{10}^2\right)}{\left(1-R_{10}\right)^2 \left(1-R_{10}R_{12}\right)^2 \left(1-R_{12}^2 e^{-\alpha\ell}\right)} \right] + \ln \frac{I'_T}{I_T} \right\} \tag{9}$$

An approximation to (9) differing in cases of interest by about 1% is the following

$$\alpha = \frac{1}{\ell} \left\{ \ln \left[\frac{\left(1-R_{12}\right)^2 \left(1-R_{10}^2\right)^2}{\left(1-R_{10}\right)^2 \left(1-R_{10}R_{12}\right)^2} \right] + \ln \frac{I'_T}{I_T} \right\} \tag{10}$$

This formula was used in the reduction of data. Its suitability was checked by comparing the resulting absorption coefficient of liquid nitrogen with that obtained from data at two different path lengths. In this case, for path length ℓ_1, we have from equations (7) and (8)

$$\frac{I_{T,1}}{I'_{T,1}} = \frac{\left(1-R_{12}\right)^2 \left(1-R_{10}^2\right)^2 \left(1-R_{10}^2\right) e^{-\alpha \ell 1}}{\left(1-R_{10}R_{12}\right)^2 \left(1-R_{12}^2 e^{-2\alpha \ell 1}\right) \left(1-R_{10}\right)^2} \tag{11}$$

Similarly, for path length 2

$$\frac{I_{T,2}}{I'_{T,2}} = \frac{\left(1-R_{12}\right)^2 \left(1-R_{10}^2\right)^2 \left(1-R_{10}^2\right) e^{-\alpha \ell 2}}{\left(1-R_{10}R_{12}\right)^2 \left(1-R_{12}^2 e^{-2\alpha \ell 2}\right) \left(1-R_{10}\right)^2} \tag{12}$$

On dividing (11) by (12)

$$\frac{I_{T,1}\ I'_{T,2}}{I'_{T,1}\ I_{T,2}} = e^{-\alpha(\ell_1-\ell_2)} \cdot \frac{\left(1-R_{12}^2 e^{-2\alpha \ell_2}\right)}{\left(1-R_{12}^2 e^{-2\alpha \ell_1}\right)} \tag{13}$$

Again, the quotient on the right hand side of equation (13) is very close to unity regardless of the value of α so that, in this case, the data reduction formula would be

$$\alpha = \frac{1}{\ell_1-\ell_2} \ln \frac{I'_{T,1}\ I_{T,2}}{I_{T,1}\ I'_{T,2}} \tag{14}$$

The absorption coefficient of liquid nitrogen was calculated from equation (10) for data from a path length of 25.4 mm and from equation (14) for data from path lengths of 25.4 mm and 4.1 mm. With

the absorption coefficient reaching a maximum value of 1.1cm $^{-1}$ a maximum discrepancy of 0.03 cm^{-1} resulted between the two methods. This was considered to be within experimental error and so the less tedious approach of measurement at a single path length was adopted for all other liquids. It may be appreciated that any error involved is of less consequence with polyethylene windows with their lower refractive index than with quartz.

In order to use equation (10) data were required for the various reflectances involved. The reflectance of the quartz windows in a vacuum was measured in a separate apparatus at liquid nitrogen temperature; the reflectance of high density polyethylene was calculated from published figures (MIT, 1957) for the dielectric constant using the Fresnel equation for normal incidence. Since polyethylene, like quartz, has a low absorption coefficient throughout the far infrared it is sufficient to use microwave measurements of the dielectric constant, ϵ, and to assume a frequency independent refractive index. However a correction must be made for low temperatures on account of the large temperature dependence of density (Corruccini and Gniewek, 1961). This was done assuming invariance of the Clausius-Mossotti function, $\frac{\epsilon - 1}{\epsilon + 2} \cdot \frac{1}{p}$, with changes in density.

To calculate the reflectance at a window/liquid interface, it is necessary to know the relative refractive index of the window material to the liquid. Again the absolute refractive index of all liquids measured could be obtained from published values of the microwave or d.c. dielectric constant (Stewart, 1964; Guillien, 1938; Werner and Keesom, 1926; van Itterbeek and Spaepen, 1943; and McLennan, et al., 1930) since these are all weakly absorbing materials. The absolute refractive index of the quartz was calculated from its reflectance while that for polyethylene we already had from its dielectric constant.

3.2 Errors

Systematic errors in calculating the absorption coefficient arise from non-linearity of the detector-amplifier-recorder system, from scattered light, and from errors in path length measurement. Non-linearity has been checked and found to be within 0.3 percent. Scattered light is a function of frequency and can best be checked by measuring the transmitted signal of a sample at a frequency where complete extinction is known to occur. However, a randomly selected test frequency does not exhaust the possibilities for scattered light.

Some indication of scattered light was available from two of our experimental runs in which complete extinction occurred. In the first, parahydrogen gave complete extinction at 390 cm^{-1} in a path length of 32.5 mm. At this frequency, the signal could not be distinguished from that with slits closed and the scattered light is therefore estimated to be less than 0.3 percent. However, because of the width of the parahydrogen absorption peak, this figure conservatively only applies to that component of the scattered light arising from incomplete filtering of higher order radiation, i.e., radiation of higher frequencies reflected by the grating in second and higher orders.

A second run in which complete extinction occurred was with liquid methane in the frequency range 70 to 250 cm^{-1} in a path length of 25.4 mm. In this range scattered light was generally less than 1 percent although an occassional point as bad as 6 percent appeared. Again this was a very broad ($\sim$ 200 cm^{-1}) band and conclusions must be conservatively limited to higher order radiation.

Our findings are in general agreement with the manufacturer's specifications which state that scattered light is less than 1 percent between 32 and 665 cm^{-1} except in the region 165 to 200 cm^{-1} where it approaches but does not exceed 4 percent. Between 20 and 32 cm^{-1}

the manufacturer gives an upper limit of 10 percent.

Path length measurements were made at room temperature with the aid of a micrometer. The major uncertainties in path length arise from shrinkage on cooling down to sample temperature and from the fact that, being in a converging-diverging beam, the infrared rays do not in general follow an axial path through the cell. The total uncertainty in path length from these causes is considered to be less than 1 percent.

Random errors in the recorded signal are by far the more serious. The situation was aggravated by the long period between recording signals with cell empty and cell full, usually as long as 1-1/2 hours. In the frequency region above 32 cm^{-1}, fluctuations in the signal of about ± 2 percent occurred in a period of five to ten minutes. Below 32 cm^{-1} fluctuations were often as great as 20 percent. It is normally not possible to average such long term fluctuations.

For all points where absorption did not exceed 50 percent the combined errors amount to 7 percent in the absorption coefficient calculated from equation (4) for frequencies above 32 cm^{-1}. Below 32 cm^{-1} the data must be regarded as of qualitative interest only. Unfortunately peak absorptions for nitrogen and hydrogen were recorded as high as 90 percent in the path lengths available. In this case the error is dominated by the scattered light problem, but an upper limit of 15 percent can be set.

The experimental absorption coefficients are plotted against wave number (reciprocal wavelength) in units of cm^{-1}. Wave number repeatability is estimated to be better than 1 cm^{-1}. A recent check of the manufacturers calibration of the gratings was made by recording drum readings at which higher order images of the mercury green line were incident on the exit slit of the monochromator. A worst

systematic error of 3 cm^{-1} was recorded, while for most of the spectrum it was less than 1 cm^{-1}. The error is hardly significant for the broad bands recorded here, particularly since the spectral slit width was sometimes as high as 10 cm^{-1}.

4. DISCUSSION

The molecular species investigated in this work have one thing in common: they are of zero or low polarity (carbon monoxide has a small permanent electric dipole moment; oxygen has an even smaller magnetic dipole moment. With these two exceptions they show no infrared absorption spectra in the gaseous state at low pressures. At higher pressures, say, of the order of 100 atmospheres, some of the far infrared spectra observed are qualitatively similar to those observed here (Bosomworth and Gush, 1965) and it is fairly well established that they have their origin in collision-induced dipoles. This has one undesirable consequence: as with other properties dependent on collisions there is no theory applicable at densities encountered in the liquid state. At this stage, therefore, a discussion must remain fairly qualitative.

Our data for liquid hydrogen at wave numbers between 20 and 250 cm^{-1} are new as are those for liquids oxygen, carbon monoxide and methane. The far infrared spectrum of liquid nitrogen and that part of the spectrum of liquid hydrogen above 300 cm^{-1} have been published previously (Stone and Williams, 1965 and Kiss, 1959).

4.1 Liquid Hydrogen

The spectrum of liquid hydrogen is the most interesting since it consists of two distinct parts each of which is strongly dependent on the ortho-para composition. The weak band below 250 cm^{-1} (figure 8) is discussed elsewhere (Jones, 1969). It is considered to be a

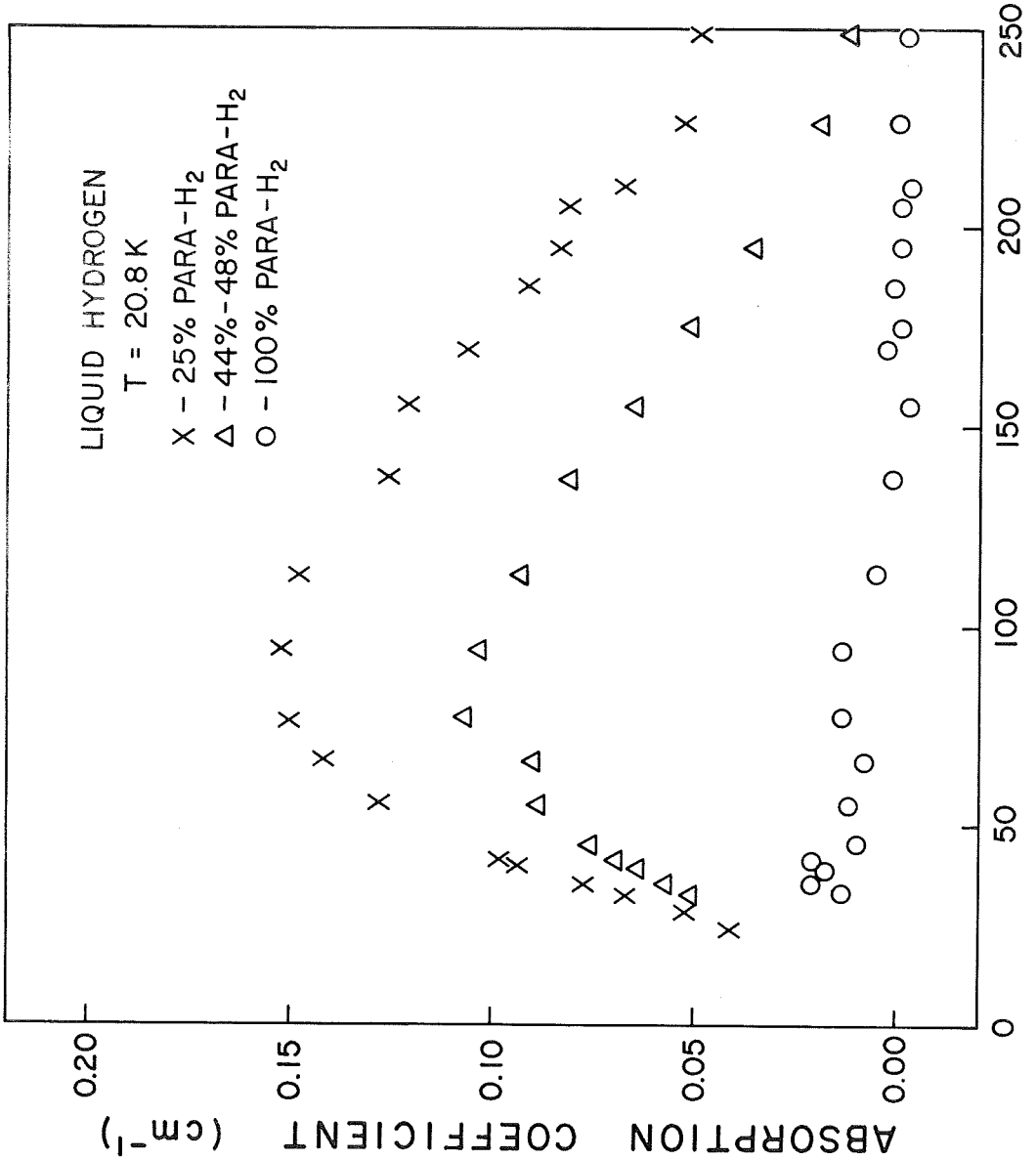

Figure 8. Far Infrared Absorption in Liquid Hydrogen-Translational Band.

translational band and its intensity is roughly linear with the concentration of ortho molecules in accordance with theory. Above 300 cm^{-1} (figure 9) is a strong band having a peak at 390 cm^{-1}. This has been identified previously as arising from the pure rotational transition from the state J=0 to J=2 of the para molecules (Kiss 1959). We were unfortunately not able to record the second maximum observed by Kiss at about 600 cm^{-1} attributable to the ortho transition J=1→3 since this was the high frequency limit of our polyethylene windows.

The results of Kiss differ slightly from the present results. While the J=0→2 band is of typically Lorentzian shape in our case — although somewhat asymmetric — Kiss's spectrum shows a pronounced shoulder close to the low density Raman frequency of 354 cm^{-1} (Stoicheff, 1957). Furthermore, Kiss also gives spectra for the solid and then the shoulder becomes a very narrow line (<4 cm^{-1} width) shifted only 1.2 cm^{-1} from the Raman frequency. Apparently our resolution was poorer and we were not able to show the two components of this band, namely: a pure rotational line and a translational summation band according to Kiss.

A discrepancy also exists in the value of the maximum absorption coefficient at 390 cm^{-1}. For para-hydrogen our peak absorption is some 40% higher while for normal hydrogen it is 30% lower than Kiss's results. These discrepancies are well outside our estimate of experimental uncertainty and remain unexplained.

4.2 Liquid Nitrogen

Our spectrum for liquid nitrogen (figure 10) is quite similar to that obtained by Stone and Williams differing only in the magnitude of the peak absorption coefficient. The values of 1.08 and 1.66 cm^{-1} respectively differ by far more than the total uncertainty estimated

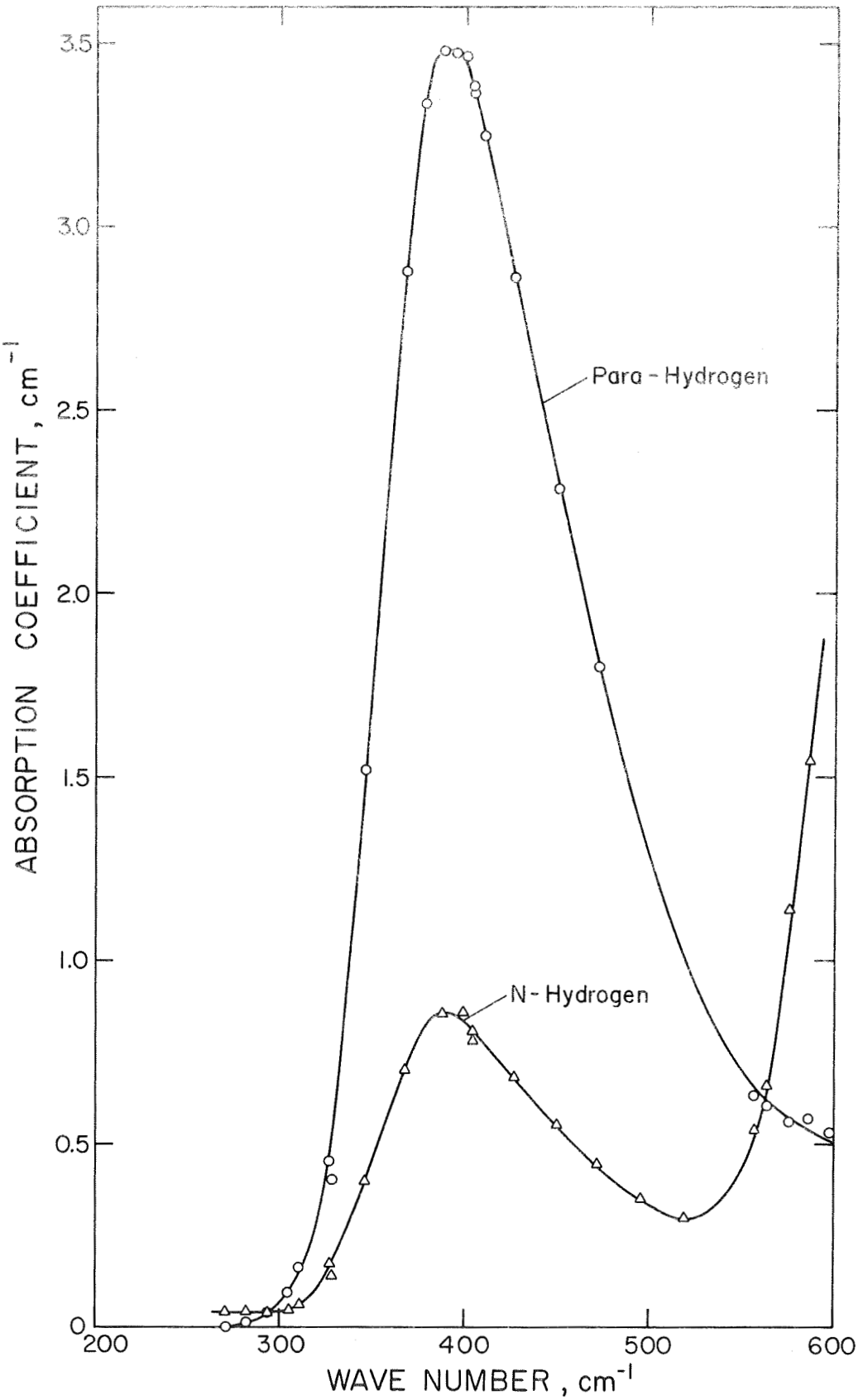

Figure 9. Far Infrared Absorption in Liquid Hydrogen-Rotational Band.

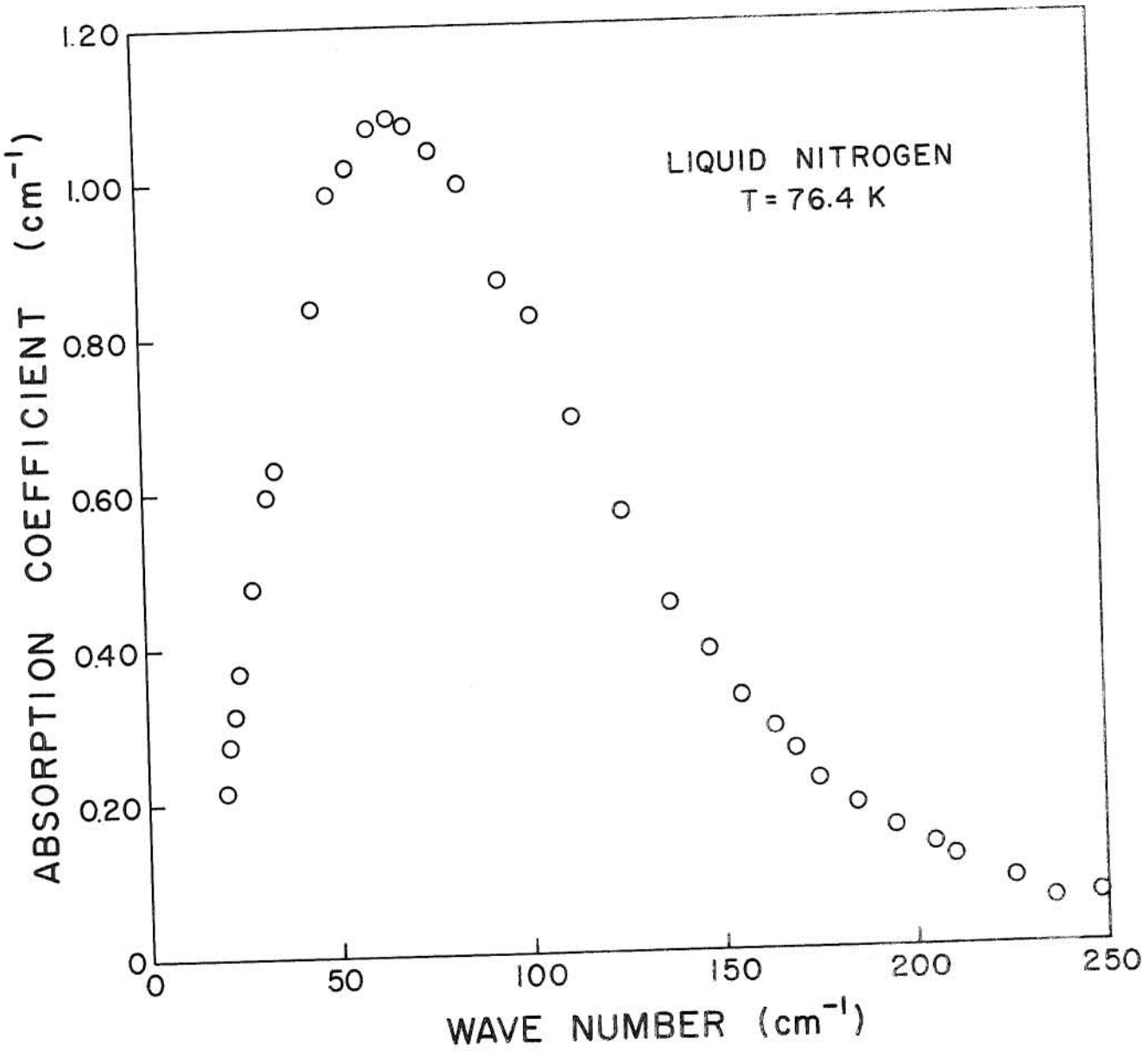

Figure 10. Far Infrared Absorption in Liquid Nitrogen.

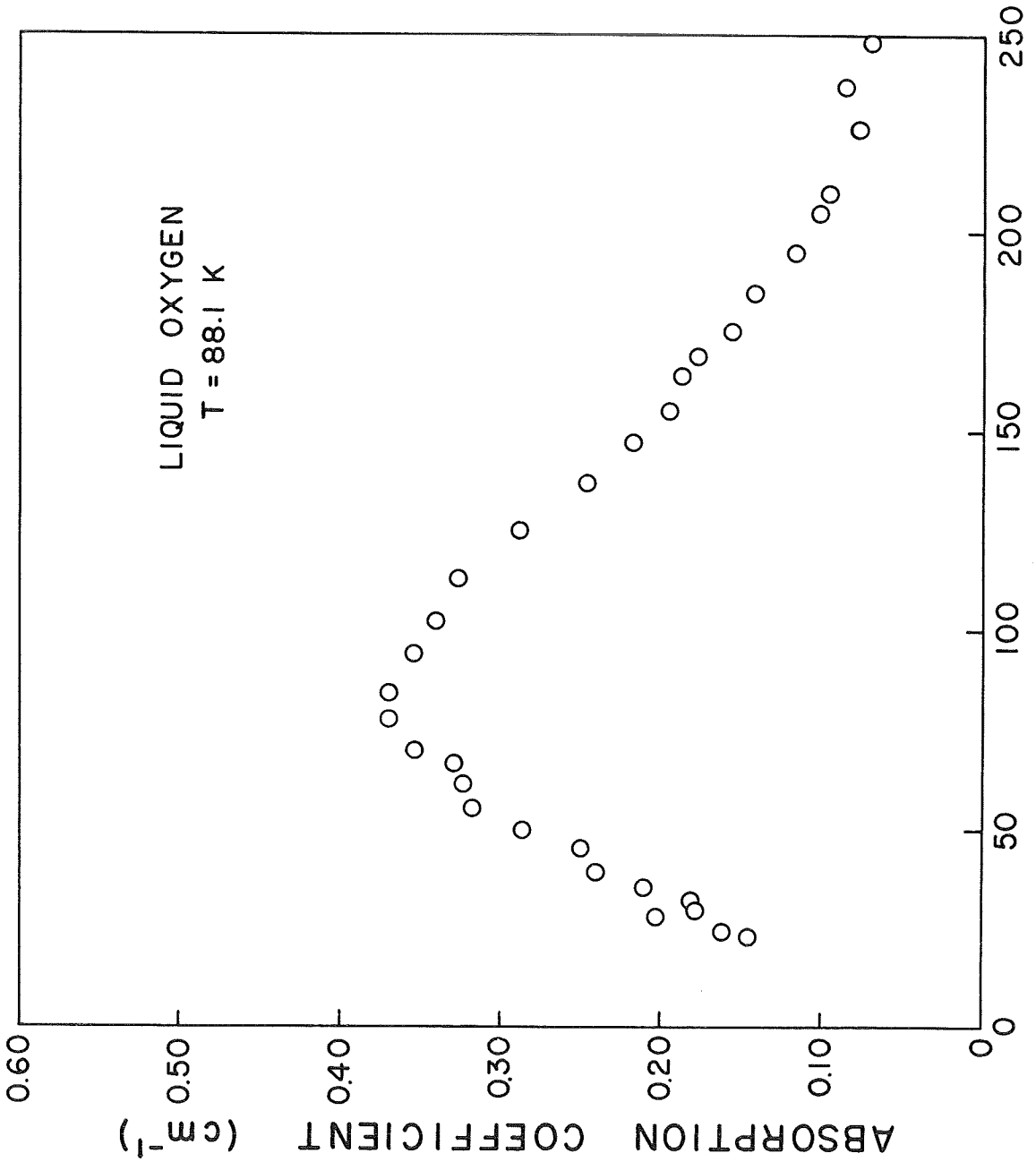

Figure 11. Far Infrared Absorption in Liquid Oxygen.

for our data. A possible explanation may lie in the difficulties mentioned by Stone and Williams in connection with the presence of ice crystals in their liquid samples. We too encountered such difficulties in earlier experiments which showed large absorption peaks at intervals over the entire spectrum. We feel that in the present data this problem has been entirely eliminated by the method of sample preparation described above.

The band is quite similar to that observed for compressed nitrogen gas (Bosomworth and Gush, 1965) for which a quadrupole-induced pure rotational origin is fairly well accepted. The broad rotational lines are more closely spaced than in the case of hydrogen (For the selection rule $\Delta J=2$ these are 8.0 cm^{-1} and 230 cm^{-1} respectively) and a large number of them are superimposed to form a continuous band.

Bearing in mind the low density limitations of existing theory one can make a crude calculation of band shape based on the binary absorption coefficient. To do this one superimposes individual broadened lines of similar shape with relative intensities given, for example, by the formula of Colpa and Ketelaar (1958). We have done this using the asymmetric line shape suggested by Kiss and Welsh (1959) with a half width at half intensity of 20 cm^{-1} (Ketelaar and Rettschnick, 1964). The calculated band does not give a good fit at all frequencies but predicts the band maximum fairly well; we calculate 60 cm^{-1} compared to about 65 cm^{-1} from experiment.

4.3 Liquid Oxygen

The spectrum of liquid oxygen, Figure 11, is quite similar to that of liquid nitrogen. However, the peak absorption coefficient is only 1/3 of that for nitrogen and the width of the band is greater. This difference was also noted by Bosomworth and Gush (1965) for the compressed gases. They point out that the difference is related to the weaker

quadrupole moment of the oxygen molecule and the resultant weaker induced dipole moment. In Table I the quantity $Q\bar{\alpha}/\sigma^4$ is listed for different molecules. Here Q is the quadrupole moment, $\bar{\alpha}$ the mean polarizability and σ the molecular diameter parameter of the Lennard-Jones potential function. This quantity is a useful measure of the induced dipole moment and the relative magnitudes of the absorption coefficient in figures 10 and 11 are in accord.

An explanation is demanded by the presence of a permanent magnetic dipole moment for oxygen, also listed in Table I. Rotational spectra in this wavelength region have been observed in the low pressure gas (Gebbie et al 1969) and attributed to magnetic dipole transitions. From the value given in Table I one might expect the resulting absorption coefficient in the liquid to be even greater than that shown for nitrogen in figure 10. But in fact these magnetic dipole rotational transitions are "approximately forbidden" and the value of the magnetic dipole itself does not tell the complete story; in order to observe them Gebbie et al used a path length of 180 m and the pure oxygen gas pressure was 3 atm. Assuming linearity of intensity with density the equivalent liquid path would be about 600 mm compared to 25.4 mm used here. Thus the magnetic dipole transitions appear to give only a minor contribution in figure 11. Similarly, in Gebbie's measurements the collision-induced transitions would have contributed only a minor part of the intensity because this part varies as the square of the density.

An envelope was again calculated as for nitrogen, but here a half width of 50 cm^{-1} was required in order to obtain a maximum at the observed frequency of 80 cm^{-1}.

Table I.

Comparison of induced and permanent dipole moments.

	Quadrupole Moment, Q 10^{-26} esu	Mean Polarizability, $\bar{\alpha}$ 10^{-25} cm^3	Lennard-Jones Force Constant, σ 10^{-8} cm	Induced Dipole, $\mu = \frac{Q\bar{\alpha}}{\sigma^4}$ 10^{-18} esu	Permanent Dipole, μ 10^{-18} esu	Rotational Constant, B_e cm^{-1}
H_2	0.63	7.9	2.968	0.0064	0	60.8
N_2	1.5	17.6	3.681	0.014	0	2.01
O_2	<0.55	16.0	3.433	0.0064	0,0185**	1.45
CO	1.6	19.5	3.590	0.019	0.112	1.93
CH_4	0	26.0	3.822	0.012*	0	5.2

* Calculated from the octopole moment, $\Omega = 3.7 \times 10^{-34}$ esu., i.e., $\mu = \frac{\Omega\bar{\alpha}}{\sigma^5}$

** Permanent magnetic dipole of 2 Bohr magnetons.

Hirschfelder, et.al., (1964).

Herzberg (1950).

Nelson, et.al., (1967).

Spurling, et.al., (1968).

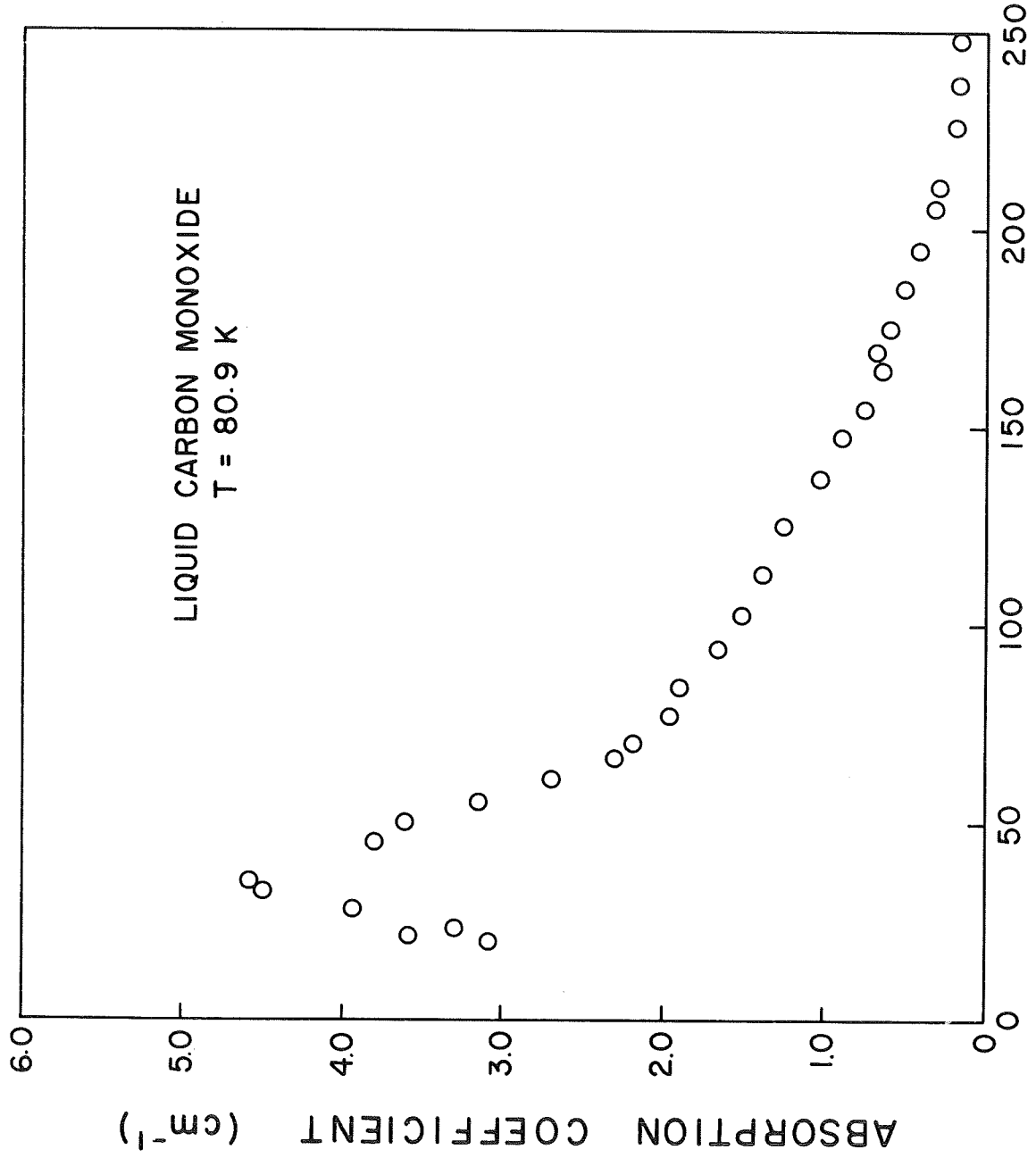

Figure 12. Far Infrared Absorption in Liquid Carbon Monoxide.

4.4 Liquid Carbon Monoxide

The far infrared spectrum of liquid carbon monoxide, Figure 12, is composed of a sharp peak superimposed on a diffuse background. The carbon monoxide molecule is similar to the nitrogen molecule in that it has the same mass and the same number of electrons. In fact the molecular constants important in collision induced absorption are also similar as seen from Table I. It is thus to be expected that the spectra would also be similar, as indeed they are toward the higher frequencies. The existence of a small permanent dipole moment for CO, however, is considered to be the source of the only major difference: i.e., the sharp low frequency peak. However, even this small permanent dipole moment is an order of magnitude larger than the quadrupole-induced dipole and its effect should dominate that of the induced dipole moment. This can be seen from Table I. On account of this permanent dipole moment pure rotational absorption must take place according to the selection rule $\Delta J=1$ in addition to $\Delta J=2$ from the induced dipole. For this process, one can calculate the relative intensities of the rotational lines (Herzberg, 1950) to find the position of peak absorption. For liquid CO at 80.9 K we find the transition from $J=6$ to $J=7$ the most intense. The corresponding frequency is 27 cm^{-1} in fair agreement with the value of 35 cm^{-1} from figure 12.

4.5 Liquid Methane

The spectrum for liquid methane is presented in figure 13. Some comment on this spectrum is called for because the methane molecule has neither permanent dipole nor quadrupole moment by virtue of its tetrahedral symmetry. The lowest order multipole allowed by symmetry is the octopole and this has been calculated from theory

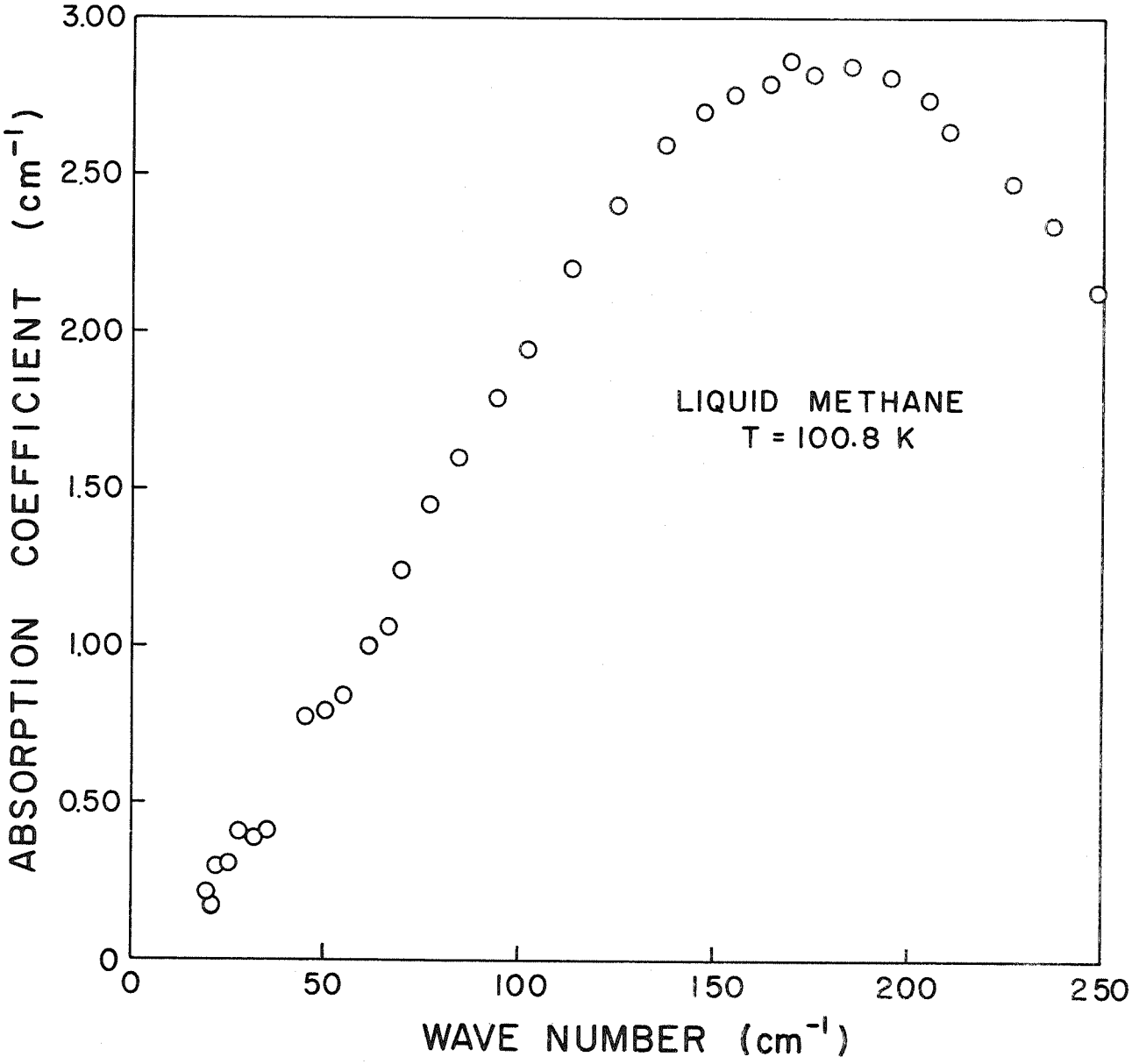

Figure 13. Far Infrared Absorption in Liquid Methane.

and from experimental second virial coefficients (Spurling, et. al., 1968). An order of magnitude estimate of the octopole-induced dipole moment at the point of closest approach of two molecules can be made from the quantity $\Omega\bar{\alpha}/\sigma^5$ (see Table I). The results would lead one to expect pure rotational absorption intensities comparable to those observed for nitrogen and thus we conclude that it is entirely feasible that the spectrum arises primarily from collision octopole-induced pure rotational transitions.

Since our measurements were completed the far infrared spectrum of compressed methane gas at room temperature has been published by Birnbaum and Rosenberg (1968) who have calculated the octopole moment from their data. Their spectrum is similar in form to ours but as would be expected for pure rotation at a higher temperature it is more intense and the maximum is at a higher frequency.

4.6 Liquid Argon

At wave numbers below 250 cm^{-1} no significant difference could be observed in the transmission through path lengths of 4.1 mm and 25.4 mm. We conclude that compared with the other five liquids studied the absorption coefficient is negligible. This is in accord with the findings of Kiss and Welsh (1959) for compressed noble gases at room temperature and up to 180 atm. pressure and wave numbers greater than 300 cm^{-1}. It is also in accord with the theory of induced absorption (Poll and van Kranendonk, 1961); no induced dipole can result from the collision of identical noble gas atoms.

5. APPLICATIONS-ABSORPTION OF THERMAL RADIATION

From a practical point of view it is of interest to be able to describe the absorption of thermal radiation in a liquid or dense vapor. Unfortunately this becomes involved with system parameters related

to the sources of radiation. However to illustrate how this might be done in a typical case we calculate here the modified Planck mean absorption coefficient (Sparrow and Cess, 1966) defined as

$$K_P(T_F,\ T) \equiv \frac{\int_0^\infty \alpha(n,\ T_F)\, I_b\,(n,\ T)\, dn}{\int_0^\infty I_b\,(n,\ T)\, dn}$$

Here n is the wave number and $I_b\,(n,\ T)$ is the black body spectral intensity for temperature T. This quantity is the correct mean absorption coefficient in optically thin conditions for incident black body radiation of temperature T when the fluid is at temperature T_F. The quantity calculated when $T = T_F$ is the Planck mean absorption coefficient and is seen to be a property of the fluid alone; i.e., contains no system parameters. However, this quantity is only of interest in emission, and, in the present, case at low temperatures is of little use. The modified coefficient as defined here contains only one system parameter, T.

For a typical problem we take T = 300 K and calculate K_P(20 K, 300 K) for liquids para and normal hydrogen. To do this with the data of figures 7 and 8 it is necessary to make an extrapolation on the high frequency side. We have determined that the high frequency side of the para-hydrogen J=0 line is representable by the Lorentz line profile within experimental error as has been observed frequently in connection with rotational lines. Thus we have extrapolated using the relation

$$\alpha\,(n) = \frac{b^2\, \alpha_{max}}{(n - n_o)^2 + b^2}$$

where α_{max} is the maximum value of the absorption coefficient at the line center, n_o, and b is the half width (86 cm^{-1}). For normal hydrogen we have had to estimate α_{max} for the J=1 line, the peak of which was not observable in our experiments. We have taken the same ratio for the J=1 line to the J=0 line as observed by Kiss, i.e., 1.88:1. The integrals were evaluated numerically and were carried to a high enough wave number that the residual contribution became negligible.

For para-hydrogen we calculate K_P = 0.53 cm^{-1} and for normal hydrogen K_P = 0.40 cm^{-1}. Thus for para-hydrogen 63% of the radiation is absorbed in a path length of 1.9 cm, while for normal hydrogen the same absorption occurs in a path length of 2.5 cm. It will be appreciated that for oxygen, nitrogen and carbon monoxide absorption of thermal radiation will be considerably less since only a narrow wave number region is covered by the observed spectra. Liquid methane on the other hand would appear to be an intermediate case. It is interesting to note that the fundamental band of liquid hydrogen in the range 4000 - 5000 cm^{-1} only accounts for at most 3 parts per million of the 300 K black body radiation and is thus of negligible importance in radiative transfer from such a source compared to the far infrared band described here.

6. CONCLUSIONS

We have measured the far infrared absorption coefficient of six cryogenic liquids at temperatures close to their normal boiling temperatures. A variety of behavior was found which could be mostly related to the molecular constants which determine the induced electric dipole moment. No theoretical relationship is available to calculate the absorption coefficient at liquid densities, but the data as such should be useful in applications such as the calculation of absorption of thermal

radiation. As an example of this the modified Planck mean absorption coefficient was calculated for normal and para-hydrogen and a 300 K source.

7. ACKNOWLEDGMENTS

The work on hydrogen was sponsored by the National Aeronautics and Space Administration, Space Nuclear Propulsion Office, under contract R-45.

The assistance of Patricia J. Giarratano is gratefully acknowledged for her help with the experiments and with data reduction. The loyal assistance of F. W. Windmoeller was also greatly appreciated.

8. REFERENCES

Birnbaum, G. and A. Rosenberg (1968), Collision induced absorption in gaseous CH_4 and CD_4 in the far infrared region, Physics Letters 27A, no. 5, 272-273.

Bosomworth, D. R. and H. P. Gush (1965), Collision-induced absorption of compressed gases in the far infrared, Part II, Canadian Journal of Physics 43, 751-769.

Colpa, J. P. and J. A. A. Ketelaar (1958), The pressure-induced rotational absorption spectrum of hydrogen: II, Molecular Physics 1, 343-357.

Corruccini, R. J. and J. J. Gniewek (1961), Thermal expansion of technical solids at low temperatures, National Bureau of Standards Monograph 29, p. 14.

Guillien, R. (1938), Sur la variation de la constante diélectrique á la solidification des liquides homopolaires, Comptes Rondues 207, 393-395.

Gebbie, H. A., W. J. Burroughs and G. R. Bird (1969), Magnetic dipole rotation spectrum of oxygen, Proc. Roy. Soc. A.310, 579-590.

Gush, H. P., W. F. J. Hare, E. J. Allin, and H. L. Welsh (1960), The infrared fundamental band of liquid and solid hydrogen, Canadian Journal of Physics 38, 176-193.

Herzberg, G. (1950), Molecular spectra and molecular structure, I. Spectra of diatomic molecules. (D. Van Nostrand Co., Inc., Princeton, New Jersey).

Hirschfelder, J. A., C. F. Curtiss, and R. B. Bird (1954), Molecular theory of gases and liquids (John Wiley and Sons, Inc., New York, N. Y.), pp. 1028, 1110, and 1111.

Jones, M. C., Far infrared absorption in liquid hydrogen, Journal of Chemical Physics 51, no. 9, 3833-3834.

Ketelaar, J. A. A. and R. P. H. Rettschnick (1964), The quadrupole moment of nitrogen deduced from the pressure-induced rotational spectrum of nitrogen, Molecular Physics 7, 191-193.

Kiss, Z. J., and H. L. Welsh (1959), The pressure-induced rotational absorption spectrum of hydrogen, II. Analysis of the absorption profile, Canadian Journal of Physics 37, 1249-1259.

Kiss, Z. J., and H. L. Welsh (1959), Pressure-induced infrared absorption of mixtures of rare gases, Physical Review Letters 2, no. 4, 166-168.

Kiss, Z. J. (1959), The rotational absorption spectrum of hydrogen, thesis submitted for the degree of Doctor of Philosophy, University of Toronto, Toronto, Canada.

Tables of dielectric materials Vol. 5, Technical Report 119, (April 1957) Laboratory for Insulation Research, Massachusetts Institute of Technology.

Mc Lennan, J. D., R. C. Jacobsen, and J. O. Wilhelm (1930), Dielectric constants of liquefied gases, Transactions of the Royal Society (Canada) 24, 37-46.

Nelson, R. D., D. R. Lide, and A. A. Marryott (1967), Selected values of electric dipole moments for molecules in the gas phase, National Standard Reference Data Series — National Bureau of Standards 10. p. 15.

Poll, J. D., and J. van Kranendonk (1961), Theory of translational absorption in gases, Canadian Journal of Physics 39, 189-204.

Sparrow, E. M., and R. D. Cess (1966), Radiation heat transfer, (Brooks/Cole Publishing Co. Belmont, California).

Spurling, T. H., A. G. DeRocco, and T. S. Storvida (1968), Intermolecular Forces in Globular Molecules, VI. Octopole Moments of Tetrahedral Molecules, Journal of Chemical Physics 48, 1006-1008.

Stewart, J. W. (1964), The dielectric polarizability of fluid parahydrogen, Journal of Chemical Physics 40, 3297.

Stoicheff, B. P. (1957), High resolution Raman spectroscopy of gases IX. Spectra of H_2, HD and D_2. Canadian Journal of Physics 35, 730-741.

Stone, N. B. W. and D. Williams (1965), Far infrared absorption in liquid nitrogen, Molecular Physics 10, 85-86.

van Itterbeek, A. and J. Spaepen (1943), Mésures sur la constante diélectrique de quelques gas non polaires (H_2, D_2, He, O_2, et l'air) et CO entre la temperature ordinaire at 20°Abs., Physica 10, 173-184.

van Kranendonk, J. and Z. J. Kiss (1959), Theory of the pressure-induced rotational spectrum of hydrogen, Canadian Journal of Physics 37, 1187-1198.

Werner, W., and W. H. Keesom (1926), The variation of the dielectric constant of liquid oxygen with temperature, Verslag. Afdeel. Naturk. Kon. Akad. Wetenschap. Amsterdam 35, 18-25.

GPO 857-506

NBS TECHNICAL PUBLICATIONS

PERIODICALS

JOURNAL OF RESEARCH reports National Bureau of Standards research and development in physics, mathematics, chemistry, and engineering. Comprehensive scientific papers give complete details of the work, including laboratory data, experimental procedures, and theoretical and mathematical analyses. Illustrated with photographs, drawings, and charts.

Published in three sections, available separately:

• Physics and Chemistry

Papers of interest primarily to scientists working in these fields. This section covers a broad range of physical and chemical research, with major emphasis on standards of physical measurement, fundamental constants, and properties of matter. Issued six times a year. Annual subscription: Domestic, $9.50; foreign, $11.75*.

• Mathematical Sciences

Studies and compilations designed mainly for the mathematician and theoretical physicist. Topics in mathematical statistics, theory of experiment design, numerical analysis, theoretical physics and chemistry, logical design and programming of computers and computer systems. Short numerical tables. Issued quarterly. Annual subscription: Domestic, $5.00; foreign, $6.25*.

• Engineering and Instrumentation

Reporting results of interest chiefly to the engineer and the applied scientist. This section includes many of the new developments in instrumentation resulting from the Bureau's work in physical measurement, data processing, and development of test methods. It will also cover some of the work in acoustics, applied mechanics, building research, and cryogenic engineering. Issued quarterly. Annual subscription: Domestic, $5.00; foreign, $6.25*.

TECHNICAL NEWS BULLETIN

The best single source of information concerning the Bureau's research, developmental, cooperative and publication activities, this monthly publication is designed for the industry-oriented individual whose daily work involves intimate contact with science and technology—*for engineers, chemists, physicists, research managers, product-development managers, and company executives.* Annual subscription: Domestic, $3.00; foreign, $4.00*.

* Difference in price is due to extra cost of foreign mailing.

NONPERIODICALS

Applied Mathematics Series. Mathematical tables, manuals, and studies.

Building Science Series. Research results, test methods, and performance criteria of building materials, components, systems, and structures.

Handbooks. Recommended codes of engineering and industrial practice (including safety codes) developed in cooperation with interested industries, professional organizations, and regulatory bodies.

Special Publications. Proceedings of NBS conferences, bibliographies, annual reports, wall charts, pamphlets, etc.

Monographs. Major contributions to the technical literature on various subjects related to the Bureau's scientific and technical activities.

National Standard Reference Data Series. NSRDS provides quantitive data on the physical and chemical properties of materials, compiled from the world's literature and critically evaluated.

Product Standards. Provide requirements for sizes, types, quality and methods for testing various industrial products. These standards are developed cooperatively with interested Government and industry groups and provide the basis for common understanding of product characteristics for both buyers and sellers. Their use is voluntary.

Technical Notes. This series consists of communications and reports (covering both other agency and NBS-sponsored work) of limited or transitory interest.

Federal Information Processing Standards Publications. This series is the official publication within the Federal Government for information on standards adopted and promulgated under the Public Law 89–306, and Bureau of the Budget Circular A–86 entitled, Standardization of Data Elements and Codes in Data Systems.

CLEARINGHOUSE

The Clearinghouse for Federal Scientific and Technical Information, operated by NBS, supplies unclassified information related to Government-generated science and technology in defense, space, atomic energy, and other national programs. For further information on Clearinghouse services, write:

Clearinghouse
U.S. Department of Commerce
Springfield, Virginia 22151

Order NBS publications from:

Superintendent of Documents
Government Printing Office
Washington, D.C. 20402

U.S. DEPARTMENT OF COMMERCE
WASHINGTON, D.C. 20230

OFFICIAL BUSINESS

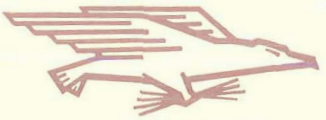

POSTAGE AND FEES PAID
U.S. DEPARTMENT OF COMMERCE